

Scalable randomized benchmarking of quantum computers using mirror circuits

Timothy Proctor, Stefan Seritan, Kenneth Rudinger, Erik Nielsen, Robin Blume-Kohout, and Kevin Young
*Quantum Performance Laboratory, Sandia National Laboratories,
 Albuquerque, NM 87185, USA and Livermore, CA 94550, USA*
 (Dated: December 21, 2021)

The performance of quantum gates is often assessed using some form of randomized benchmarking. However, the existing methods become infeasible for more than approximately five qubits. Here we show how to use a simple and customizable class of circuits — randomized mirror circuits — to perform scalable, robust, and flexible randomized benchmarking of Clifford gates. We show that this technique approximately estimates the infidelity of an average many-qubit logic layer, and we use simulations of up to 225 qubits with physically realistic error rates in the range 0.1-1% to demonstrate its scalability. We then use experiments on up to 16 qubits to demonstrate that our technique can reveal and quantify crosstalk errors in many-qubit circuits.

Quantum information processors suffer from a wide variety of errors that must be quantified if their performance is to be understood and improved. A processor’s errors are commonly probed using randomized benchmarks that involve running random circuits [1–22] — e.g., standard randomized benchmarking (RB) [3, 4] or one of its many variants [3–18], cross-entropy benchmarking [19], or the quantum volume benchmark [22]. Randomized benchmarks are appealing because they aggregate many kinds of error into one number that quantifies average performance over a large circuit ensemble. Unlike tomographic techniques [23] that estimate a set of parameters that may be exponentially large in the number of qubits (n), randomized benchmarks hold the potential for scalable performance assessment.

Yet current randomized benchmarks have one of two scaling problems. Quantum volume and cross-entropy benchmarking require classical computations that are exponentially expensive in n , becoming infeasible beyond $n \sim 50$ [19–22]. In contrast, standard RB requires only efficient classical computations but it benchmarks composite gates from the n -qubit Clifford group. They require $O(n^2/\log n)$ two-qubit gates to implement [24–26], so the fidelity of a typical n -qubit Clifford decreases quickly with n . This makes standard RB on more than a few qubits currently infeasible. Standard RB has only been implemented on up to three qubits [27], and even its streamlined variant “direct RB” has only been implemented on up to 5 qubits [17].

In this Letter we introduce a simple, flexible, and robust RB method that removes the Clifford compilation bottleneck that limits current methods. Our technique is based on *circuit mirroring* [28], a recently introduced framework for constructing scalable benchmarks. We show how *randomized mirror circuits* (Fig. 1a) enable scalable RB of Clifford gates. They can be used to estimate the infidelity of an average Pauli-dressed [29–32] n -qubit circuit layer (Fig. 1a, grey boxes). Mirror RB can be applied whenever a typical n -qubit circuit layer has significantly non-zero fidelity, enabling RB of hundreds or even thousands of qubits with physically realistic error rates [$O(10^{-2})$ - $O(10^{-3})$]. We demonstrate and validate mirror RB with simulations on up to 225 qubits (Fig. 2), and experiments on up to 16 qubits (Figs. 1, 3 and 4).

Randomized mirror circuits. Mirror RB is based on the *randomized mirror circuits* [28] shown in Fig. 1a. By design, each

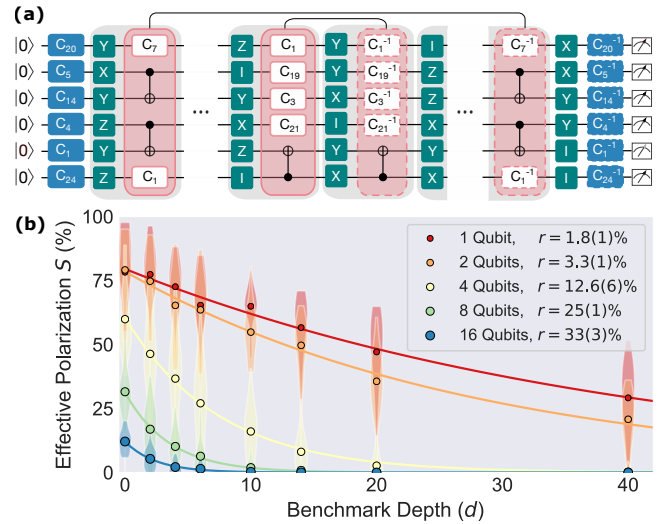


Figure 1. Scalable RB with mirror circuits. (a) Randomized mirror circuits over Clifford gates, which we use for scalable RB. These circuits contain a layer of uniformly random one-qubit Clifford gates and its inverse (blue boxes), $d + 1$ layers of uniformly random Pauli gates (green boxes), and $d/2$ pairs of layers consisting of a layer and its inverse (pink boxes) sampled from some set of n -qubit Clifford layers. The number of “Pauli-dressed” layers (grey boxes) d is the circuit’s *benchmark depth*. These circuits’ “effective polarization” S , a quantity closely related to success probability, decays exponential with d . (b) Results of experiments on 1, 2, 4, 8 and 16 qubit subsets of IBM Q Rueschlikon. Points (violin plots) are the means (distributions) of S versus d , and the curves are fits to $S = Ap^d$. Each r is a rescaling of p that approximates the infidelity of an average Pauli-dressed n -qubit layer (uncertainties are 1σ here and throughout).

randomized mirror circuit C should ideally always produce a single bit string s_C that is efficient to compute. Distributions over these circuits are parameterized by an n -qubit layer set $\mathbb{L} = \{L\}$ [33], a probability distribution Ω over \mathbb{L} , and a benchmark depth d that specifies the number of Pauli-dressed layers in the circuit. Both \mathbb{L} and Ω are customizable, but we require that (1) each layer contains only Clifford gates, (2) each layer’s inverse L^{-1} is also within \mathbb{L} [although L^{-1} does not need to be implemented using the inverse of the evolution used for L], (3) $\Omega(L) = \Omega(L^{-1})$, and (4) Ω -random layers quickly locally randomize an error (local “twirling”) and

spread it across multiple qubits. Note that condition (4) is also required for reliable direct RB, and the circumstances under which it is satisfied have been studied in detail [18]. For all simulations and experiments herein, the layer set consists of parallel applications of CNOTs between connected qubits and all 24 single-qubit Clifford gates. Generic layer sets that don't necessarily respect a processor's connectivity could be used (e.g., all-to-all CNOTs), but we don't do so here. All our distributions Ω have a similar form whereby sampling a layer consists of: (1) sampling some CNOTs, and (2) sampling uniformly random single-qubit Clifford gates for all qubits not acted on by those CNOTs.

Mirror RB. The aim of our protocol is to measure $\epsilon_\Omega := \sum_L \Omega(L) \epsilon(\bar{PL})$, where Ω is a user-chosen distribution over \mathbb{L} , and $\epsilon(\bar{PL})$ is the entanglement infidelity of the Pauli-dressed version of the n -qubit layer L (grey boxes, Fig. 1a). In our simulations and experiments we do not compile the Paulis into the L layers, but this is permissible. Our protocol estimates ϵ_Ω using data from Ω -sampled randomized mirror circuit, and the following novel data analysis method. For each circuit C that we run, we estimate its *effective polarization*

$$S = \frac{4^n}{4^n - 1} \left[\sum_{k=0}^n \left(-\frac{1}{2} \right)^k h_k \right] - \frac{1}{4^n - 1}, \quad (1)$$

where h_k is the probability that the circuit outputs a bit string that is a Hamming distance of k from its target bit string (s_C). As our theory (below) shows, the simple additional analysis in computing S mitigates the limited “twirling” enacted by our circuits.

Our protocol — “mirror RB” — retains the simplicity of standard RB: we fit data to an exponential, and extract an error rate (r_Ω) from the estimated decay rate (p). Mirror RB is the following:

1. For a range of integers $d \geq 0$, sample K randomized mirror circuits that have a benchmark depth of d , using the sampling distribution Ω , and run each one $N \geq 1$ times.
2. Estimate each circuit's effective polarization S .
3. Fit \bar{S}_d , the mean of S at benchmark depth d , to $\bar{S}_d = Ap^d$, where A and p are fit parameters, and then compute $r_\Omega = (4^n - 1)(1 - p)/4^n$ as an estimate of ϵ_Ω .

Theory. We now show that mirror RB is reliable, i.e., $\bar{S}_d \approx Ap^d$ and $r_\Omega \approx \epsilon_\Omega$ under broad conditions. We assume that errors are Markovian [34], but not necessarily gate-independent. We use $U(L)$ and $\phi(L)$ to denote the n -qubit superoperators that represent a layer L 's perfect and imperfect implementations, respectively, and $\mathcal{E}(L)$ its error map, i.e., $\phi(L) = \mathcal{E}(L)U(L)$. Our theory starts from a single randomized mirror circuit C of benchmark depth d . So $C = F_0^{-1}P_dL_1^{-1} \cdots P_{1+d/2}L_{d/2}^{-1}P_{d/2}L_{d/2} \cdots P_1L_1P_0F_0$, where (1) P_i are Pauli layers, (2) F_0 and F_0^{-1} consist of one-qubit Clifford gates, and (3) L_i are Ω -sampled layers and L_i^{-1} their inverses. The components (1), (2) and (3) are sampled independently.

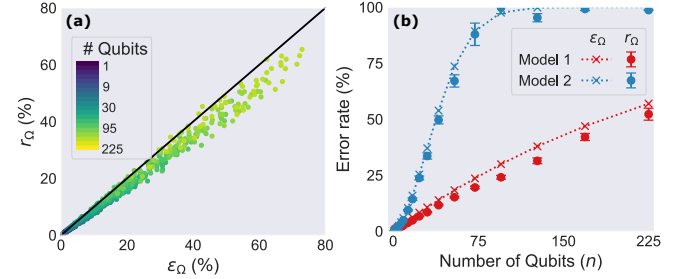


Figure 2. **Validating mirror RB with 100+ qubit simulations.** Simulations of mirror RB on up to 225 qubits show that it reliably approximates the infidelity of n -qubit layers, i.e., $r_\Omega \approx \epsilon_\Omega$. (a) r_Ω versus ϵ_Ω for randomly sampled error models. Each point was generated from an independent simulation (sampling an error model and circuits, simulating the circuits, and then applying the analysis to estimate r_Ω) for gates subject to stochastic Pauli errors. (b) r_Ω and ϵ_Ω versus n for two illustrative error models, with (model 2) and without (model 1) long-range crosstalk. This demonstrates the power of mirror RB to highlight crosstalk errors.

To compute a formula for \bar{S}_d we can therefore average over (1-3) separately in turn [even though when we sample circuits we do not, e.g., take multiple samples of (1) for each sample of (1-2) and so on].

First we calculate the effect of averaging over the Pauli layers (green boxes, Fig. 1a). They are independent, uniformly random, and interleaved between every other layer. They therefore have two effects: they randomize the target bit string (s), which guarantees that $\bar{S}_d \rightarrow 0$ as $d \rightarrow \infty$ to a good approximation [35], and they twirl the errors on the L_i layers into stochastic Pauli errors [29–32]. So we can analyze the “residual” circuit $C = F_0^{-1}L_1^{-1} \cdots L_d^{-1}L_d \cdots L_1F_0$ with each L_i 's error map $\mathcal{E}(L_i)$ a stochastic Pauli channel (that includes a contribution from errors in the Pauli layers). The composite superoperator for this circuit is $\phi(C) = \phi(F_0^{-1})\mathcal{E}_d\phi(F_0)$ where $\mathcal{E}_d \equiv \phi(L_1^{-1}) \cdots \phi(L_d^{-1})\phi(L_d) \cdots \phi(L_1)$ is a stochastic Pauli channel, as each $U(L_i)$ is a Clifford operator.

Next we calculate the effect of averaging over the initial and final Clifford layers (blue boxes, Fig. 1a). The initial layer F_0 contains independent, uniformly random single-qubit Clifford gates. Therefore this averaging implements *local 2-design* twirling on each qubit [36]. That is, $\bar{\mathcal{E}}_d \equiv \frac{1}{2^{4n}} \sum_{F_0} [U(F_0^{-1})\mathcal{E}_d U(F_0)]$ is a stochastic Pauli channel with equal *marginal* probabilities to induce an X , Y or Z error on any fixed qubit (this holds approximately when there are errors in F_0 and F_0^{-1} [37–40]). An error induced by $\bar{\mathcal{E}}_d$ flips at least one output bit iff it applies X or Y to at least one qubit. So, if $\bar{\mathcal{E}}_d$ induces a weight k error (an error on k qubits) the circuit outputs s_C with a probability of $1/3^k$. Generally, a weight k error causes flips on j of the output bits with probability $M_{jk} = \binom{j}{k} \frac{2^j}{3^k}$. So $\bar{h} = M\vec{p}$ where h_k and p_k are the probabilities that k bits are flipped and that $\bar{\mathcal{E}}_d$ induces a weight k error, respectively, with $k = 0, \dots, n$. By inverting M , we obtain $p_0 = \sum_{k=0}^n (-1/2)^k h_k \equiv H$, and note that $p_0 = 1 - \epsilon(\mathcal{E}_d)$ where $\epsilon(\mathcal{E}_d)$ is \mathcal{E}_d 's entanglement infidelity. So H equals \mathcal{E}_d 's entanglement fidelity $1 - \epsilon(\mathcal{E}_d)$, and S [Eq. (1)] its polarization

tion $\gamma(\mathcal{E}_d) := 1 - 4^n \epsilon(\mathcal{E}_d)/(4^n - 1)$. State preparation and measurement (SPAM) errors also contribute to S (and H), as do errors in F_0 and F_0^{-1} . But their effect is approximately d -independent, so $S \approx A\gamma(\mathcal{E}_d)$ for some A .

We have related a randomized mirror circuit's S to the polarization of its superoperator $[\gamma(\mathcal{E}_d)]$. Now we relate $\gamma(\mathcal{E}_d)$ to the polarizations of the circuit's constituent layers $[\gamma(\mathcal{E}(L_i))]$. If every $\mathcal{E}(L_i)$ is an n -qubit depolarizing channel, with layer-dependent error rates, then $\gamma(\mathcal{E}_d) = \prod_{i=1}^d \gamma_{i^{-1}} \gamma_i$ where $\gamma_i \equiv \gamma(\mathcal{E}(L_i))$. More generally this will not hold exactly, but we argue that $\gamma(\mathcal{E}_d) \approx \prod_{i=1}^d \gamma_{i^{-1}} \gamma_i$ for a typical randomized mirror circuit. For two stochastic Pauli channels \mathcal{E}_1 and \mathcal{E}_2 , $\gamma(\mathcal{E}_1 \mathcal{E}_2) = \gamma(\mathcal{E}_1)\gamma(\mathcal{E}_2) + \eta$ where $\eta = (4^n - 1)^2 \text{Cov}(\vec{\epsilon}_1, \vec{\epsilon}_2)$, $\vec{\epsilon}_i$ is the vector of $4^n - 1$ Pauli error probabilities for \mathcal{E}_i , and Cov is the covariance. η quantifies the rate that errors cancel when composing the two channels, relative to the rate that they cancel when composing n -qubit depolarization channels. It is negligible unless $\vec{\epsilon}_1$ and $\vec{\epsilon}_2$ are sparse (e.g., if $\vec{\epsilon}_1 = \vec{\epsilon}_2$ and the error probability is equal distributed over K errors, then $\eta = \epsilon(\mathcal{E}_1)^2 \left[\frac{1}{K} - \frac{1}{4^n - 1} \right]$). So, unless the Pauli error probability distributions of the L_i are sharply spiked, then $\gamma(\mathcal{E}_d) \approx \prod_{i=1}^d \gamma_{i^{-1}} \gamma_i$ for any randomized mirror circuit. Furthermore, because of the properties that we demand of Ω (see above), our circuits are “scrambling”—they locally randomize errors, and they quickly spread any error across many qubits. This suppresses error cancellation further [17, 18]. So $\gamma(\mathcal{E}_d) \approx \prod_{i=1}^d \gamma_{i^{-1}} \gamma_i$ for a typical randomized mirror circuit.

Finally, we calculate the effect of averaging over the L_i layers (pink boxes, Fig. 1a). They are sampled independently from Ω , so $\bar{S}_d \approx A(\sum_L \Omega(L) \gamma_{L^{-1}} \gamma_L)^{d/2}$ where $\gamma_L \equiv \gamma(\mathcal{E}(L))$. That is, $\bar{S}_d \approx A p^d$ where $p^2 \approx \sum_L \Omega(L) \gamma_{L^{-1}} \gamma_L$. Rewriting this in terms of ϵ_Ω and $\text{Cov}_\Omega = [\sum_L \Omega(L) \epsilon(L^{-1}) \epsilon(L)] - [\epsilon_\Omega]^2$ gives $p^2 \approx (1 - \frac{4^n}{4^n - 1} \epsilon_\Omega)^2 + \frac{4^n}{4^n - 1} \text{Cov}_\Omega$. So if $\text{Cov}_\Omega = 0$ then $r_\Omega \approx \epsilon_\Omega$. Cov_Ω quantifies the correlation between the error rate of a Ω -random layer L and its inverse L^{-1} , so $\text{Cov}_\Omega \neq 0$ is likely. This covariance satisfies $\epsilon_\Omega(1 - \epsilon_\Omega) \geq \text{Cov}_\Omega \geq -\epsilon_\Omega^2$, so $\epsilon_\Omega + O(\epsilon_\Omega^2) \gtrapprox r_\Omega \gtrapprox \frac{\epsilon_\Omega}{2} + O(\epsilon_\Omega^2)$. Therefore r_Ω is never significantly large than ϵ_Ω , and it can be smaller by at most a factor of ≈ 2 . The $\{\epsilon(L)\}$ distributions required to get close to these bounds on Cov_Ω are not physically typical, e.g., the upper bound is saturated if $\epsilon(L) = \epsilon(L^{-1})$ and $\epsilon(L) \in \{0, 1\}$ (i.e., each layer has an error rate of 0 or 1). We therefore conjecture that, for physically relevant $\{\epsilon(L)\}$, r_Ω typically only slightly underestimates ϵ_Ω . This is supported by our simulations and experiments.

Simulations. We simulated our protocol on 1-225 qubits with randomly sampled stochastic Pauli error models. The qubits were arranged on a 15×15 lattice (the layer set is described above). We independently sampled many RB experiments, for a range of $n \in [1..225]$ (totaling 900 RB experiments). We used a distribution Ω whereby a layer sampled from Ω has an expected CNOT density of $1/8$. For each RB experiment we sampled a different error model, consisting of biased and correlated Pauli errors with one- and two-qubit gates having an expected infidelity of 0.1% and 1%, respectively [41]. Fig. 2a shows ϵ_Ω versus r_Ω . We observe that $r_\Omega \approx \epsilon_\Omega$, with r_Ω typically slightly less than ϵ_Ω , as expected from our the-

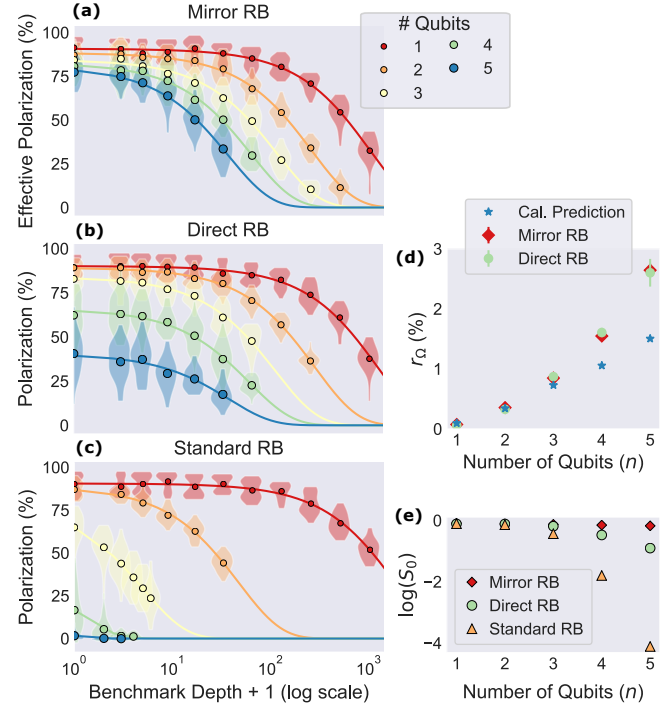


Figure 3. Experimental validation of mirror RB. Mirror, direct and standard RB on 1-5 qubits of IBM Q Quito. (a-c) The means (points) and distributions (violin plots) of the circuit polarizations versus benchmark depth (d), and fits to an exponential Ap^d (curves), for mirror, direct and standard RB. (d) The error rates (r) obtained from the fit's decay rate for direct and mirror RB versus the number of qubits (n), and the values predicted from calibration data. The direct and mirror RB error rates are in close agreement, validating mirror RB against the reliable but unscalable direct RB protocol. The measured r diverges from the predictions of Quito's calibration data as n increases, indicating crosstalk. (e) The mean polarizations at $d = 0$ (S_0) decrease rapidly with n for direct/standard RB [at best $\log(S_0) = 1 - O(n^2/\log n)$] making them infeasible beyond a few qubits, whereas $\log(S_0) = 1 - O(n)$ for mirror RB.

ory. Quantifying estimation error by $\delta_{\text{rel}} = \frac{r_\Omega - \epsilon_\Omega}{\epsilon_\Omega}$, we find that $\delta_{\text{rel}} > -0.32$ in all 900 simulations and for each n its mean $\bar{\delta}_{\text{rel}}$ satisfies $0.003 > \bar{\delta}_{\text{rel}} > -0.16$. Although this systematic underestimation of ϵ_Ω is undesirable, it is arguably small enough to be insignificant (particularly as RB is typically used for rough estimates of gate performance rather than precision characterization).

To show how our protocol can be used to reveal crosstalk errors, we simulated it on our hypothetical 225-qubit processor with two illustrative models: (1) a crosstalk-free model and (2) a long-range crosstalk model. The crosstalk-free model consisted of 0.5% readout error on each qubit, and depolarization on the one- and two-qubit gates, with 0.1% and 1% error rates, respectively. In the crosstalk model, each CNOT also caused the error probability for qubit q to increase by $\epsilon(q)$, with $\epsilon(q)$ a slowly decreasing function of the distance (on the lattice) from q to the CNOT location [41]. Fig. 2b shows r_Ω (points) and ϵ_Ω (dotted line) versus n for both models. We find that $r_\Omega \approx \epsilon_\Omega$ (averaged over n), $\bar{\delta}_{\text{rel}} \approx -0.17$ and $\bar{\delta}_{\text{rel}} \approx -0.08$

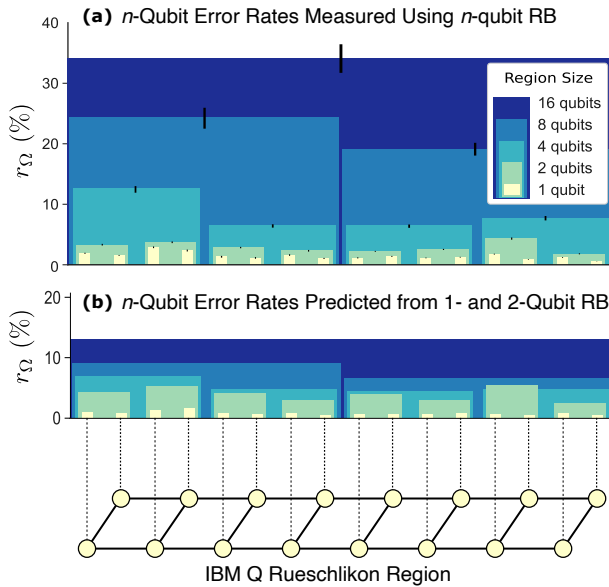


Figure 4. Mapping out the performance of a 16-qubit processor. Mirror RB was used to probe the performance of n -qubit regions of IBM Q Rueschlikon. (a) The measured error rate (r_Ω) for each qubit subset that was tested (black lines are 1σ uncertainties) and (b) the over-optimistic predictions from calibration data. The horizontal axis is a device schematic (nodes are qubits and edges the available CNOTs).

for the crosstalk-free and crosstalk models, respectively), and that r_Ω grows quadratically at low n under the crosstalk model — an effect that cannot be observed without running many-qubit circuits.

Experimental validation of mirror RB. To demonstrate mirror RB and compare it to existing techniques, we ran mirror, direct [17] and standard [3] RB on 1-5 qubits of IBM Q Quito [42]. Direct RB is designed to measure the same quantity as mirror RB (ϵ_Ω) and is known to be reliable but unscalable (because its circuits start by preparing a random n -qubit stabilizer state). For direct and mirror RB we sampled layers with an expected CNOT density of $\xi = 1/8$ [41] (standard RB does not have flexible sampling and its error rate is incomparable). Fig. 3a-c shows that we observe exponential decays for all three methods and all n (for all methods $d = 0$ corresponds to the shortest allowed circuit, consisting of a random n -qubit Clifford and its inverse for standard RB and preparation in and measurement of a random stabilizer state for direct RB). For standard and direct RB we rescale the success probabilities P to polarizations $(P - 1/2^n)/(1 - 1/2^n)$ [this has no effect on the estimated r] for easier comparison with mirror RB. Fig. 3a-c also highlights the fundamentally improved scaling of mirror RB. The $d = 0$ polarization (Fig. 3e) decays much more quickly with n for direct and standard RB, because they use subroutines containing $O(n^2/\log n)$ gates, whereas $d = 0$ randomized mirror circuits use $O(n)$ gates. We find that the error rates estimated by direct and mirror RB are in close agreement for all n (Fig. 3d), which is a clear experimental validation of mirror RB. We also predicted r_Ω from Quito’s calibration data

(obtained from one- and two-qubit standard RB) [41]. These predictions (stars, Fig. 3d) are consistent with our observations for $n = 1, 2$, but they are over-optimistic as n increases. This discrepancy is a clear sign of crosstalk errors, induced by CNOT gates (the one-qubit calibration data is obtained from running one-qubit RB simultaneously [36, 42], so those error rates include contributions from any one-qubit gate crosstalk).

Mapping out a processor’s performance. Quantum computer users often want to identify the best n qubits within a larger processor [43]. Our protocol can be used to map out performance of a processor’s n -qubit layers when varying both n and the embedding of those qubits, as we demonstrate on IBM Q Rueschlikon (16 qubits) [42]. For $n \in \{1, 2, 4, 8, 16\}$ we divided Rueschlikon into $16/n$ regions, and ran randomized mirror circuits on each region (the one-qubit experiments were performed simultaneously to match the calibration experiments) [41]. In this experiment, we fixed the expected number of CNOTs in a layer to $1/2$. Fig. 1b shows exponential decays for one region of each size (the leftmost regions in Fig. 4), and Figs. 4a and 4b show r_Ω for all benchmarked regions and the predictions from the calibration data, respectively. The prediction underestimates r_Ω for $n > 2$ (as with IBM Q Quito), again signifying crosstalk induced by CNOTs.

Discussion. RB experiments are ubiquitous, but to date they have been restricted to five or fewer qubits. In this Letter we have introduced a technique that opens the door to holistic RB of $n \gg 1$ qubits, because it is feasible on hundreds or thousands of qubits. Yet it retains the core simplicity of standard RB — fitting data from random circuits to an exponential. Many RB techniques have been built on the unscalable foundations of standard RB, e.g., methods for estimating the error rates of individual gates [10, 44, 45], for quantifying coherent errors [46–48], for estimating leakage [49–51], for calibrating gates [52, 53], and for quantifying crosstalk [14, 36]. We anticipate that many of these techniques can be improved using the methods introduced here. For example, because mirror RB does not require compilation of subroutines it removes the circuit scheduling complexities that plague simultaneous standard RB [14, 36], suggesting that mirror RB will be a more powerful and flexible tool for probing crosstalk. Similarly, because mirror RB’s circuits have user-specified sampling, running multiple mirror RB experiments with Ω varied could be used to isolate the error rates of different subsets of layers and/or gates [17].

Our experiments revealed and quantified crosstalk errors that are invisible to one- and two-qubit RB, highlighting the need for scalable methods like ours. Outside the paradigm of RB there are a variety of existing methods for testing n -qubit circuit layers, and our technique complements them. For example, cycle benchmarking [32, 54] and Pauli noise estimation [55, 56] can characterize a Pauli-dressed n -qubit layer. These techniques extract more information about a layer’s errors, but, unlike mirror RB, they test only one (or a few) of a processor’s many possible n -qubit layers. Applying analysis techniques like those in Refs. [54–56] to extract more information from randomized mirror circuit data is an intriguing possibility.

Our method is built on a particular type of randomized mirror circuits, but circuit mirroring [28] is a flexible tool for constructing scalable benchmarks, and it could be used to construct different kinds of “randomized mirror circuits”. We anticipate that this flexibility can be exploited to construct a range of RB protocols and other random circuit benchmarks with complementary properties to ours. For example, it is possible to construct mirror circuits that contain non-Clifford gates [28], suggesting a route to scalable RB of universal gate sets — and even scalable “full stack” benchmarks.

Since the completion of this manuscript, Mayer *et al.* [57] presented a complementary theory for mirror RB that assumed gate-independent errors and used a less sophisticated data analysis routine.

Data and code availability. All data and analysis code are available at 10.5281/zenodo.5197714. Our circuit sampling code is available in pyGSTi [58, 59].

Acknowledgements: This work was supported by the Laboratory Directed Research and Development program at Sandia National Laboratories and the U.S. Department of Energy, Office of Science, Office of Advanced Scientific Computing Research through the Quantum Testbed Program. Sandia National Laboratories is a multi-program laboratory managed and operated by National Technology and Engineering Solutions of Sandia, LLC., a wholly owned subsidiary of Honeywell International, Inc., for the U.S. Department of Energy’s National Nuclear Security Administration under contract DE-NA-0003525. All statements of fact, opinion or conclusions contained herein are those of the authors and should not be construed as representing the official views or policies of the U.S. Department of Energy, or the U.S. Government, or the views of IBM. We thank the IBM Q team for technical support.

REFERENCES

- [1] Joseph Emerson, Robert Alicki, and Karol Źyczkowski, “Scalable noise estimation with random unitary operators,” *J. Opt. B Quantum Semiclass. Opt.* **7**, S347 (2005).
- [2] Joseph Emerson, Marcus Silva, Osama Moussa, Colm Ryan, Martin Laforest, Jonathan Baugh, David G Cory, and Raymond Laflamme, “Symmetrized characterization of noisy quantum processes,” *Science* **317**, 1893–1896 (2007).
- [3] Easwar Magesan, Jay M Gambetta, and Joseph Emerson, “Scalable and robust randomized benchmarking of quantum processes,” *Phys. Rev. Lett.* **106**, 180504 (2011).
- [4] Easwar Magesan, Jay M Gambetta, and Joseph Emerson, “Characterizing quantum gates via randomized benchmarking,” *Phys. Rev. A* **85**, 042311 (2012).
- [5] Emanuel Knill, D Leibfried, R Reichle, J Britton, RB Blakestad, JD Jost, C Langer, R Ozeri, S Seidelin, and DJ Wineland, “Randomized benchmarking of quantum gates,” *Phys. Rev. A* **77**, 012307 (2008).
- [6] Arnaud Carignan-Dugas, Joel J Wallman, and Joseph Emerson, “Characterizing universal gate sets via dihedral benchmarking,” *Phys. Rev. A* **92**, 060302 (2015).
- [7] Andrew W Cross, Easwar Magesan, Lev S Bishop, John A Smolin, and Jay M Gambetta, “Scalable randomised benchmarking of non-clifford gates,” *NPJ Quantum Inf.* **2**, 16012 (2016).
- [8] Winton G. Brown and Bryan Eastin, “Randomized benchmarking with restricted gate sets,” *Phys. Rev. A* **97**, 062323 (2018).
- [9] A. K. Hashagen, S. T. Flammia, D. Gross, and J. J. Wallman, “Real randomized benchmarking,” *Quantum* **2**, 85 (2018).
- [10] Easwar Magesan, Jay M Gambetta, Blake R Johnson, Colm A Ryan, Jerry M Chow, Seth T Merkel, Marcus P da Silva, George A Keefe, Mary B Rothwell, Thomas A Ohki, *et al.*, “Efficient measurement of quantum gate error by interleaved randomized benchmarking,” *Phys. Rev. Lett.* **109**, 080505 (2012).
- [11] Jonas Helsen, Xiao Xue, Lieven MK Vandersypen, and Stephanie Wehner, “A new class of efficient randomized benchmarking protocols,” *arXiv preprint arXiv:1806.02048* (2018).
- [12] Jonas Helsen, Sepehr Nezami, Matthew Reagor, and Michael Walter, “Matchgate benchmarking: Scalable benchmarking of a continuous family of many-qubit gates,” (2020), *arXiv:2011.13048 [quant-ph]*.
- [13] Jahan Claes, Eleanor Rieffel, and Zhihui Wang, “Character randomized benchmarking for non-multiplicity-free groups with applications to subspace, leakage, and matchgate randomized benchmarking,” (2020), *arXiv:2011.00007 [quant-ph]*.
- [14] David C McKay, Andrew W Cross, Christopher J Wood, and Jay M Gambetta, “Correlated randomized benchmarking,” (2020), *arXiv:2003.02354 [quant-ph]*.
- [15] Jonas Helsen, Ingo Roth, Emilio Onorati, Albert H Werner, and Jens Eisert, “A general framework for randomized benchmarking,” (2020), *arXiv:2010.07974 [quant-ph]*.
- [16] A Morvan, V V Ramasesh, M S Blok, J M Kreikebaum, K O’Brien, L Chen, B K Mitchell, R K Naik, D I Santiago, and I Siddiqi, “Qutrit randomized benchmarking,” (2020), *arXiv:2008.09134 [quant-ph]*.
- [17] Timothy J Proctor, Arnaud Carignan-Dugas, Kenneth Rudinger, Erik Nielsen, Robin Blume-Kohout, and Kevin Young, “Direct randomized benchmarking for multiqubit devices,” *Phys. Rev. Lett.* **123** (2019).
- [18] Timothy J Proctor, Arnaud Carignan-Dugas, Erik Nielsen, Kenneth Rudinger, Robin Blume-Kohout, and Kevin Young, “Direct randomized benchmarking: robust and flexible benchmarking of quantum gates,” In preparation (2021).
- [19] Sergio Boixo, Sergei V Isakov, Vadim N Smelyanskiy, Ryan Babbush, Nan Ding, Zhang Jiang, Michael J Bremner, John M Martinis, and Hartmut Neven, “Characterizing quantum supremacy in near-term devices,” *Nat. Phys.* **14**, 595 (2018).
- [20] Frank Arute, Kunal Arya, Ryan Babbush, Dave Bacon, Joseph C Bardin, Rami Barends, Rupak Biswas, Sergio Boixo, Fernando GSL Brandao, David A Buell, *et al.*, “Quantum supremacy using a programmable superconducting processor,” *Nature* **574**, 505–510 (2019).
- [21] Yunchao Liu, Matthew Otten, Roozbeh Bassirianjahromi, Liang Jiang, and Bill Fefferman, “Benchmarking near-term quantum computers via random circuit sampling,” (2021), *arXiv:2105.05232 [quant-ph]*.
- [22] Andrew W Cross, Lev S Bishop, Sarah Sheldon, Paul D Nation, and Jay M Gambetta, “Validating quantum computers using randomized model circuits,” *Phys. Rev. A* **100**, 032328 (2019).
- [23] Erik Nielsen, John King Gamble, Kenneth Rudinger, Travis Scholten, Kevin Young, and Robin Blume-Kohout, “Gate set tomography,” (2020), *arXiv:2009.07301 [quant-ph]*.
- [24] Scott Aaronson and Daniel Gottesman, “Improved simulation of stabilizer circuits,” *Phys. Rev. A* **70**, 052328 (2004).
- [25] Ketan N Patel, Igor L Markov, and John P Hayes, “Efficient

synthesis of linear reversible circuits,” *Quantum Inf. Comput.* **8**, 282–294 (2008).

[26] Sergey Bravyi and Dmitri Maslov, “Hadamard-free circuits expose the structure of the clifford group,” *arXiv preprint arXiv:2003.09412* (2020).

[27] David C McKay, Sarah Sheldon, John A Smolin, Jerry M Chow, and Jay M Gambetta, “Three qubit randomized benchmarking,” *Phys. Rev. Lett.* **122**, 200502 (2019).

[28] Timothy Proctor, Kenneth Rudinger, Kevin Young, Erik Nielsen, and Robin Blume-Kohout, “Measuring the capabilities of quantum computers,” *arXiv preprint arXiv:2008.11294* (2020).

[29] E Knill, “Quantum computing with realistically noisy devices,” *Nature* **434**, 39–44 (2005).

[30] Joel J Wallman and Joseph Emerson, “Noise tailoring for scalable quantum computation via randomized compiling,” *Phys. Rev. A* **94**, 052325 (2016).

[31] Matthew Ware, Guilhem Ribeill, Diego Ristè, Colm A Ryan, Blake Johnson, and Marcus P da Silva, “Experimental demonstration of pauli-frame randomization on a superconducting qubit,” (2018), *arXiv:1803.01818 [quant-ph]*.

[32] Akel Hashim, Ravi K Naik, Alexis Morvan, Jean-Loup Ville, Bradley Mitchell, John Mark Kreikebaum, Marc Davis, Ethan Smith, Costin Iancu, Kevin P O’Brien, Ian Hincks, Joel J Wallman, Joseph Emerson, and Irfan Siddiqi, “Randomized compiling for scalable quantum computing on a noisy superconducting quantum processor,” (2020), *arXiv:2010.00215 [quant-ph]*.

[33] n -qubit layers are also known as cycles or n -qubit gates.

[34] Erik Nielsen, John King Gamble, Kenneth Rudinger, Travis Scholten, Kevin Young, and Robin Blume-Kohout, “Gate set tomography,” *arXiv preprint arXiv:2009.07301* (2020).

[35] Robin Harper, Ian Hincks, Chris Ferrie, Steven T Flammia, and Joel J Wallman, “Statistical analysis of randomized benchmarking,” *Physical Review A* **99**, 052350 (2019).

[36] Jay M Gambetta, AD Córcoles, Seth T Merkel, Blake R Johnson, John A Smolin, Jerry M Chow, Colm A Ryan, Chad Rigetti, S Poletto, Thomas A Ohki, *et al.*, “Characterization of addressability by simultaneous randomized benchmarking,” *Phys. Rev. Lett.* **109**, 240504 (2012).

[37] Timothy Proctor, Kenneth Rudinger, Kevin Young, Mohan Sarovar, and Robin Blume-Kohout, “What randomized benchmarking actually measures,” *Phys. Rev. Lett.* **119**, 130502 (2017).

[38] Joel J Wallman, “Randomized benchmarking with gate-dependent noise,” *Quantum* **2**, 47 (2018).

[39] Seth T Merkel, Emily J Pritchett, and Bryan H Fong, “Randomized benchmarking as convolution: Fourier analysis of gate dependent errors,” *arXiv preprint arXiv:1804.05951* (2018).

[40] Arnaud Carignan-Dugas, Kristine Boone, Joel J Wallman, and Joseph Emerson, “From randomized benchmarking experiments to gate-set circuit fidelity: how to interpret randomized benchmarking decay parameters,” *New J. Phys.* **20**, 092001 (2018).

[41] See the Supplemental Material.

[42] IBM Quantum <https://quantum-computing.ibm.com>, (2021).

[43] Prakash Murali, Jonathan M Baker, Ali Javadi-Abhari, Frederic T Chong, and Margaret Martonosi, “Noise-Adaptive compiler mappings for noisy Intermediate-Scale quantum computers,” in *Proceedings of the Twenty-Fourth International Conference on Architectural Support for Programming Languages and Operating Systems*, ASPLOS ’19 (Association for Computing Machinery, New York, NY, USA, 2019) pp. 1015–1029.

[44] Robin Harper and Steven T Flammia, “Estimating the fidelity of T gates using standard interleaved randomized benchmarking,” *Quantum Sci. Technol.* **2**, 015008 (2017).

[45] Tobias Chasseur, Daniel M Reich, Christiane P Koch, and Frank K Wilhelm, “Hybrid benchmarking of arbitrary quantum gates,” *Phys. Rev. A* **95**, 062335 (2017).

[46] Joel Wallman, Chris Granade, Robin Harper, and Steven T Flammia, “Estimating the coherence of noise,” *New J. Phys.* **17**, 113020 (2015).

[47] Guanru Feng, Joel J Wallman, Brandon Buonacorsi, Franklin H Cho, Daniel K Park, Tao Xin, Dawei Lu, Jonathan Baugh, and Raymond Laflamme, “Estimating the coherence of noise in quantum control of a solid-state qubit,” *Phys. Rev. Lett.* **117**, 260501 (2016).

[48] Sarah Sheldon, Lev S Bishop, Easwar Magesan, Stefan Philipp, Jerry M Chow, and Jay M Gambetta, “Characterizing errors on qubit operations via iterative randomized benchmarking,” *Phys. Rev. A* **93**, 012301 (2016).

[49] Christopher J Wood and Jay M Gambetta, “Quantification and characterization of leakage errors,” *Phys. Rev. A* **97**, 032306 (2018).

[50] T Chasseur and FK Wilhelm, “Complete randomized benchmarking protocol accounting for leakage errors,” *Phys. Rev. A* **92**, 042333 (2015).

[51] Joel J Wallman, Marie Barnhill, and Joseph Emerson, “Robust characterization of loss rates,” *Phys. Rev. Lett.* **115**, 060501 (2015).

[52] MA Rol, CC Bultink, TE O’Brien, SR de Jong, LS Theis, X Fu, F Luthi, RFL Vermeulen, JC de Sterke, A Bruno, *et al.*, “Restless tuneup of high-fidelity qubit gates,” *Phys. Rev. Appl.* **7**, 041001 (2017).

[53] J Kelly, R Barends, B Campbell, Y Chen, Z Chen, B Chiaro, A Dunsworth, AG Fowler, I-C Hoi, E Jeffrey, *et al.*, “Optimal quantum control using randomized benchmarking,” *Phys. Rev. Lett.* **112**, 240504 (2014).

[54] Alexander Erhard, Joel James Wallman, Lukas Postler, Michael Meth, Roman Stricker, Esteban Adrian Martinez, Philipp Schindler, Thomas Monz, Joseph Emerson, and Rainer Blatt, “Characterizing large-scale quantum computers via cycle benchmarking,” *Nat. Commun.* **10**, 5347 (2019).

[55] Robin Harper, Steven T. Flammia, and Joel J. Wallman, “Efficient learning of quantum noise,” *Nat. Phys.* **16**, 1–5 (2020).

[56] Steven T. Flammia and Joel J. Wallman, “Efficient estimation of Pauli channels,” *ACM Trans. Quant. Comp.* **1**, 3 (2020).

[57] Karl Mayer, Alex Hall, Thomas Gatterman, Si Khadir Halit, Kenny Lee, Justin Bohnet, Dan Gresh, Aaron Hankin, Kevin Gilmore, and John Gaebler, “Theory of mirror benchmarking and demonstration on a quantum computer,” *arXiv [quant-ph]* (2021), *arXiv:2108.10431 [quant-ph]*.

[58] Erik Nielsen, Kenneth Rudinger, Timothy Proctor, Antonio Russo, Kevin Young, and Robin Blume-Kohout, “Probing quantum processor performance with pyGSTi,” *Quantum Sci. Technol.* **5**, 044002 (2020).

[59] Erik Nielsen, Robin Blume-Kohout, Lucas Saldyt, Jonathan Gross, Travis Scholten, Kenneth Rudinger, Timothy Proctor, and John King Gamble, “PyGSTi version 0.9.9.1,” (2020), 10.5281/zenodo.3675466.

[60] Robin Blume-Kohout and Kevin C Young, “A volumetric framework for quantum computer benchmarks,” *Quantum* **4**, 362 (2020).

SUPPLEMENTAL MATERIAL

A. Simulations

Here we provide details of the simulations of mirror RB presented in the main text (see Fig. 2). All the error models that we simulated consisted of only stochastic Pauli errors. This enabled simulations that are efficient (polynomial) in the number of qubits (n). We implemented “weak” simulation using a standard stochastic unravelling, i.e., for error model M and circuit C , we sampled from $P(x | C, M)$, denoting C ’s output distribution over bit strings under error model M . Under our error models, for each layer in C , M implies a probability distribution over the n -qubit Pauli operators (encoding a stochastic Pauli channel) that specifies the probability of each Pauli occurring after that layer (so the probability of the identity is the probability of no error). To obtain a sample from $P(x | C, M)$, we sampled a Pauli operator instance after each layer in C (from M ’s error distributions) to obtain a sequence of Clifford operators. We then simulated that sampled sequence using CHP [24] (using an interface built into pyGSTi [58, 59]), obtaining a single bit string. All of our simulations consisted of generating $N = 100$ samples for each distinct circuit.

In the main text we presented the results of two distinct sets of simulations, shown in Figs. 2a and 2b. In both cases, the simulations are of n -qubit mirror RB for 18 different values of n , ranging from $n = 1$ up to $n = 225$ qubits with exponential spacing. These simulations are of an n qubit subset of 225 qubits that are arranged on a 15×15 square lattice with CNOT gates available between nearest-neighbor qubits. We independently sampled 50 distinct mirror RB experiment designs (a set of mirror RB circuits) at each n , with $K = 30$ circuits per benchmark depth. The randomized mirror circuits depend on two user-specified components: the n -qubit layer set \mathbb{L} and the sampling distribution Ω over \mathbb{L} . The layer set that we used was constructed in the same way as in all of our experiments and simulations: \mathbb{L} consisted of all parallel applications of CNOTs between connected qubits and all 24 single-qubit Clifford gates. The sampling distribution was the “edge grab” sampler, with a two-qubit gate density of $1/8$, that was introduced and described in detail in the supplemental material of Ref. [28].

Fig. 2a shows the results of simulating each of these $50 \times 18 = 900$ mirror RB experiment designs once, with an independent, randomly sampled error model for each mirror RB experiment design. For each RB experiment design, an error model was sampled as follows. The readout for each qubit is assigned a bit flip error probability, sampled uniformly and independently for each qubit from the interval $[0\%, 1\%]$. For each qubit, each of the 24 single-qubit gates (from the set of all 24 single-qubit Clifford gates) is independently assigned an n -qubit error map that acts after the gate. This error map has $3 + 3k$ error rate parameters that we sample, where k is number of neighbours for this qubit ($k = 4$ unless the qubit is on the edge of the lattice). The error map contains the 3 weight-1 Pauli errors on the target qubit, with error rates of $\{l_i\}_{i=1}^3$, and the $3k$ weight-1 Pauli errors that can occur on neighbouring

qubits, with rates $\{c_i\}_{i=1}^{3k}$. These rates are sampled as follows. We sample γ uniformly from the interval $[0\%, 0.2\%]$, κ uniformly from the interval $[0.5, 1]$, l'_i uniformly from the interval $[0, 1]$ for $i = 1, 2, 3$, and c'_i uniformly from the interval $[0, 1]$ for $i = 1, \dots, 3k$. If the gate is a σ_z -basis rotation we set $c'_i = 0$ for all i . We then set $l_i = \gamma\kappa l'_i / \sum_j l'_j$ and $c_i = \gamma(1 - \kappa)c'_i / \sum_j c'_j$. Therefore, the total rate of errors that this gate induces on its target qubit is $\epsilon_{\text{targ}} = \kappa\gamma$, and the total rate of errors that it induces on its neighbours is $\epsilon_{\text{nn}} = \gamma(1 - \kappa)$ — except for σ_z -basis rotation where $\epsilon_{\text{nn}} = 0$ (we make this choice as σ_z -basis rotation do not typically involve a physical pulse). The error map for each CNOT gate (corresponding to each edge on the lattice) is constructed in the same way, except that (1) γ is sampled uniformly from the $[0\%, 2\%]$, and (2) there are 15 possible Pauli errors on the target qubit, and so $\{l_i\}_{i=1}^{15}$. In each of the 900 independent simulations, we extract ϵ_Ω from the error model and we estimate r_Ω from the simulated data. Fig. 2a shows a scatter plot of ϵ_Ω versus r_Ω .

The simulations in Fig. 2b consisted of sampling one mirror RB experiment design for each n under two different error models — with and without long-range crosstalk errors. In the first model (model 1)

- The readout on each qubit is subject to a bit flip error with a probability of 0.5%.
- Each one-qubit gate (any one of the 24 single-qubit Clifford gates) is followed by a one-qubit depolarizing channel with an entanglement infidelity of 0.1%.
- Each CNOT gate is followed by a two-qubit depolarizing channel with an entanglement infidelity of 1%.

The second model (model 2) is the same as model 1 except that the CNOT gates also cause long-range crosstalk errors. In particular, each CNOT is still followed by a two-qubit depolarizing channel with an entanglement infidelity of 1% on its two target qubits, q_1 and q_2 , but it also causes local one-qubit depolarization on all other qubits. It applies a one-qubit depolarizing channel on qubit q with an entanglement infidelity of $\delta(q)$, where $\delta(q)$ is a decreasing function of the distance (on the lattice) from q to the CNOT location. The specific function used was $\delta(q) = 0.0035 \times 0.999^{d(q, q_1, q_2)}$ where $d(q, q_1, q_2)$ is the minimum of the distance between q and q_1 and the distance between q and q_2 . For each of the two models, at each n we extract ϵ_Ω from the error model and we estimate r_Ω from the simulated data. Fig. 2b shows ϵ_Ω and r_Ω versus n for both error models.

B. IBM Q Quito experiments

Our experiment on IBM Q Quito (ibmq_quito version 1.1.3, a 5-qubit Falcon r4T processor) was performed in June 2021. It consisted of running mirror, direct and standard RB on 1-5 qubits. Randomized mirror circuits are constructed using two user-specified components: the n -qubit layer set \mathbb{L} and the sampling distribution Ω over \mathbb{L} . The layer set that we used in this experiment was constructed in the same way as in all

of our experiments and simulations: \mathbb{L} consisted of all parallel applications of CNOTs between connected qubits and all 24 single-qubit Clifford gates. The sampling distribution was the “edge grab” sampler, with a two-qubit gate density of $1/8$, that was introduced and described in detail in the supplemental material of Ref. [28]. For each n , we used exponentially spaced benchmark depths d (see Fig. 3). For each n and d , we sampled and ran $K = 30$ randomized mirror circuits.

Direct RB [17] contains the same flexible sampling as mirror RB: the user specifies \mathbb{L} and Ω . Direct RB is designed to measure the same average layer infidelity (ϵ_Ω), but because direct RB and mirror RB are different protocols there is no a priori guarantee that their empirical error rates r_Ω will be equal. One of the motivations for running direct RB alongside mirror RB is to show that we obtain approximately the same r_Ω in both techniques. For direct RB, we therefore choose to use the same \mathbb{L} and Ω as in our concurrent mirror RB experiment.

For our purposes, an n -qubit direct RB circuit of benchmark depth d consists of (1) a circuit that generates a uniformly random n -qubit stabilizer state, (2) a sequence of d Pauli-dressed layers, consisting of a uniformly random Pauli layer and then a layer L sampled from Ω , and (3) a circuit that returns the qubits to a uniformly random computational basis state. To implement direct RB, it is necessary to compile the sub-circuits of steps (1) and (3) into the available gates (and it is the large circuits generated by this compilation when $n \gg 1$ that makes direct RB unscalable). We do so using the open-source compilers in pyGSTi. To analyze the direct RB data, we fit the mean success probability versus depth to $Ap^d + 1/2^n$, and then $r_\Omega = (4^n - 1)(1 - p)/4^n$ as with mirror RB. We are able to fix the asymptote to $1/2^n$ because the target bit string is randomized [35]. In Fig. 3 we present polarization decays, instead of success probability decays, but note that this is only a rescaling.

Our standard RB experiments follow the standard procedure for RB over the Clifford group [3, 4], except that we randomized the ideal output bit string by only inverting each sequence of random Clifford gates up to a randomly sampled Pauli operator. Although this is not current standard practice, it has been advocated for elsewhere — because it means that the success probability decay will asymptote to $1/2^n$ [35]. In particular, and as with direct RB, we fit the mean success probability versus depth to $Ap^d + 1/2^n$ (for standard RB, we use the number of Clifford subroutines minus two to define the benchmark depth d , as then the shortest circuits allowed by all three methods correspond to $d = 0$). Standard RB does not contain any flexible sampling, but it is necessary to compile the n -qubit Clifford subroutines in the circuits into the available gates. As with direct RB, we do so using the open-source compilers in pyGSTi. These compilations are unlikely

to be optimal (e.g., in the number of CNOTs in the circuits), and so a slower decrease in the $d = 0$ success probability with n (or, equivalently, a slower decrease in the $d = 0$ mean polarization \bar{S}_0 , which is what is shown in Fig. 2e) than observed in our experiment might have been achievable. However, at least $O(n^2/\log(n))$ two-qubit gates are required to implement a typical n -qubit Clifford operator [24–26], so it is not possible to improve upon the scaling seen in our experimental results.

In the main text we do not present the error rates r obtained from the standard RB experiments, as they are not directly comparable to the direct and mirror RB error rates. Specifically, standard RB measures (up to some subtleties [37–40]) the infidelity of an average n -qubit Clifford gate, whereas direct and mirror RB approximately measure ϵ_Ω — the error rate of an average layer. The observed n -qubit Clifford RB error rate r_n is $r_1 = 0.041(1)\%$, $r_2 = 1.97(5)\%$, $r_3 = 17.9(7)\%$, $r_4 = 67(6)\%$ and $r_5 = 95(7)\%$, where we have defined $r = (4^n - 1)(1 - p)/4^n$ rather than using the more common definition of $r = (2^n - 1)(1 - p)/2^n$ for consistency with the convention that we have used for mirror and direct RB (which we choose due to the arguably preferable properties of entanglement infidelity compared to average gate infidelity).

C. IBM Q Rueschlikon experiments

Our experiment on IBM Q Rueschlikon (ibmqx5 version 1.1.0, a 16-qubit processor) was performed in July 2018. It consisted of running mirror RB on multiple n -qubit subsets of the processor, for $n \in \{1, 2, 4, 8, 16\}$. For each n , we divided Rueschlikon into $16/n$ regions (as shown in Fig. 4), and we ran randomized mirror circuits on each region. The one-qubit experiments were performed simultaneously to match the calibration experiments. This experiment used a sampling distribution Ω for which sampling a layer consisted of (1) selecting a pair of connected qubits uniformly at random, and adding a CNOT between those qubits to the layer with probability 50%, and (2) sampling independent and uniformly random single-qubit Clifford gates to apply to all qubits that do not have a CNOT acting on them. A layer sampled from this Ω therefore contains no CNOT gates with 50% probability and otherwise it contains one CNOT gate. Note that this sampling distribution is not suitable for much larger processors (unlike the edge grab sampler used in our simulations and the experiments on IBM Q Quito). This is because the CNOT density $\xi \rightarrow 0$ as $n \rightarrow \infty$ and circuits containing very few two-qubit gates cannot be scrambling [18]. The data from these experiments was also presented in Ref. [28] (see Fig. 1 therein), where it was used to construct volumetric benchmarking plots [60] rather than estimate layer error rates.